Title

Search for B0→K*+K*-

Permalink

https://escholarship.org/uc/item/99k4g38g

Journal

Physical Review D, 78(5)

ISSN

2470-0010

Authors

Aubert, B
Bona, M
Karyotakis, Y
et al.

Publication Date

2008-09-01

DOI

10.1103/physrevd.78.051103

Peer reviewed

Search for $B^0 \rightarrow K^{*+}K^{*-}$

B. Aubert,[1] M. Bona,[1] Y. Karyotakis,[1] J. P. Lees,[1] V. Poireau,[1] E. Prencipe,[1] X. Prudent,[1] V. Tisserand,[1] J. Garra Tico,[2] E. Grauges,[2] L. Lopez,[3,4] A. Palano,[3,4] M. Pappagallo,[3,4] G. Eigen,[5] B. Stugu,[5] L. Sun,[5] G. S. Abrams,[6] M. Battaglia,[6] D. N. Brown,[6] R. N. Cahn,[6] R. G. Jacobsen,[6] L. T. Kerth,[6] Yu. G. Kolomensky,[6] G. Kukartsev,[6] G. Lynch,[6] I. L. Osipenkov,[6] M. T. Ronan,[6,*] K. Tackmann,[6] T. Tanabe,[6] C. M. Hawkes,[7] N. Soni,[7] A. T. Watson,[7] H. Koch,[8] T. Schroeder,[8] D. Walker,[9] D. J. Asgeirsson,[10] B. G. Fulsom,[10] C. Hearty,[10] T. S. Mattison,[10] J. A. McKenna,[10] M. Barrett,[11] A. Khan,[11] L. Teodorescu,[11] V. E. Blinov,[12] A. D. Bukin,[12] A. R. Buzykaev,[12] V. P. Druzhinin,[12] V. B. Golubev,[12] A. P. Onuchin,[12] S. I. Serednyakov,[12] Yu. I. Skovpen,[12] E. P. Solodov,[12] K. Yu. Todyshev,[12] M. Bondioli,[13] S. Curry,[13] I. Eschrich,[13] D. Kirkby,[13] A. J. Lankford,[13] P. Lund,[13] M. Mandelkern,[13] E. C. Martin,[13] D. P. Stoker,[13] S. Abachi,[14] C. Buchanan,[14] J. W. Gary,[15] F. Liu,[15] O. Long,[15] B. C. Shen,[15,*] G. M. Vitug,[15] Z. Yasin,[15] L. Zhang,[15] V. Sharma,[16] C. Campagnari,[17] T. M. Hong,[17] D. Kovalskyi,[17] M. A. Mazur,[17] J. D. Richman,[17] T. W. Beck,[18] A. M. Eisner,[18] C. J. Flacco,[18] C. A. Heusch,[18] J. Kroseberg,[18] W. S. Lockman,[18] T. Schalk,[18] B. A. Schumm,[18] A. Seiden,[18] L. Wang,[18] M. G. Wilson,[18] L. O. Winstrom,[18] C. H. Cheng,[19] D. A. Doll,[19] B. Echenard,[19] F. Fang,[19] D. G. Hitlin,[19] I. Narsky,[19] T. Piatenko,[19] F. C. Porter,[19] R. Andreassen,[20] G. Mancinelli,[20] B. T. Meadows,[20] K. Mishra,[20] M. D. Sokoloff,[20] P. C. Bloom,[21] W. T. Ford,[21] A. Gaz,[21] J. F. Hirschauer,[21] A. Kreisel,[21] M. Nagel,[21] U. Nauenberg,[21] J. G. Smith,[21] K. A. Ulmer,[21] S. R. Wagner,[21] R. Ayad,[22,+] A. Soffer,[22,‡] W. H. Toki,[22] R. J. Wilson,[22] D. D. Altenburg,[23] E. Feltresi,[23] A. Hauke,[23] H. Jasper,[23] M. Karbach,[23] J. Merkel,[23] A. Petzold,[23] B. Spaan,[23] K. Wacker,[23] M. J. Kobel,[24] W. F. Mader,[24] R. Nogowski,[24] K. R. Schubert,[24] R. Schwierz,[24] J. E. Sundermann,[24] A. Volk,[24] D. Bernard,[25] G. R. Bonneaud,[25] E. Latour,[25] Ch. Thiebaux,[25] M. Verderi,[25] P. J. Clark,[26] W. Gradl,[26] S. Playfer,[26] J. E. Watson,[26] M. Andreotti,[27,28] D. Bettoni,[27] C. Bozzi,[27] R. Calabrese,[27,28] A. Cecchi,[27,28] G. Cibinetto,[27,28] P. Franchini,[27,28] E. Luppi,[27,28] M. Negrini,[27,28] A. Petrella,[27,28] L. Piemontese,[27] V. Santoro,[27,28] R. Baldini-Ferroli,[29] A. Calcaterra,[29] R. de Sangro,[29] G. Finocchiaro,[29] S. Pacetti,[29] P. Patteri,[29] I. M. Peruzzi,[29,§] M. Piccolo,[29] M. Rama,[29] A. Zallo,[29] A. Buzzo,[30] R. Contri,[30,31] M. Lo Vetere,[30,31] M. M. Macri,[30] M. R. Monge,[30,31] S. Passaggio,[30] C. Patrignani,[30,31] E. Robutti,[30] A. Santroni,[30,31] S. Tosi,[30,31] K. S. Chaisanguanthum,[32] M. Morii,[32] J. Marks,[33] S. Schenk,[33] U. Uwer,[33] V. Klose,[34] H. M. Lacker,[34] D. J. Bard,[35] P. D. Dauncey,[35] J. A. Nash,[35] W. Panduro Vazquez,[35] M. Tibbetts,[35] P. K. Behera,[36] X. Chai,[36] M. J. Charles,[36] U. Mallik,[36] J. Cochran,[37] H. B. Crawley,[37] L. Dong,[37] W. T. Meyer,[37] S. Prell,[37] E. I. Rosenberg,[37] A. E. Rubin,[37] Y. Y. Gao,[38] A. V. Gritsan,[38] Z. J. Guo,[38] C. K. Lae,[38] A. G. Denig,[39] M. Fritsch,[39] G. Schott,[39] N. Arnaud,[40] J. Béquilleux,[40] A. D'Orazio,[40] M. Davier,[40] J. Firmino da Costa,[40] G. Grosdidier,[40] A. Höcker,[40] V. Lepeltier,[40] F. Le Diberder,[40] A. M. Lutz,[40] S. Pruvot,[40] P. Roudeau,[40] M. H. Schune,[40] J. Serrano,[40] V. Sordini,[40,‖] A. Stocchi,[40] G. Wormser,[40] D. J. Lange,[41] D. M. Wright,[41] I. Bingham,[42] J. P. Burke,[42] C. A. Chavez,[42] J. R. Fry,[42] E. Gabathuler,[42] R. Gamet,[42] D. E. Hutchcroft,[42] D. J. Payne,[42] C. Touramanis,[42] A. J. Bevan,[43] C. K. Clarke,[43] K. A. George,[43] F. Di Lodovico,[43] R. Sacco,[43] M. Sigamani,[43] G. Cowan,[44] H. U. Flaecher,[44] D. A. Hopkins,[44] S. Paramesvaran,[44] F. Salvatore,[44] A. C. Wren,[44] D. N. Brown,[45] C. L. Davis,[45] K. E. Alwyn,[46] D. S. Bailey,[46] R. J. Barlow,[46] Y. M. Chia,[46] C. L. Edgar,[46] G. D. Lafferty,[46] T. J. West,[46] J. I. Yi,[46] J. Anderson,[47] C. Chen,[47] A. Jawahery,[47] D. A. Roberts,[47] G. Simi,[47] J. M. Tuggle,[47] C. Dallapiccola,[48] X. Li,[48] E. Salvati,[48] S. Saremi,[48] R. Cowan,[49] D. Dujmic,[49] P. H. Fisher,[49] K. Koeneke,[49] G. Sciolla,[49] M. Spitznagel,[49] F. Taylor,[49] R. K. Yamamoto,[49] M. Zhao,[49] P. M. Patel,[50] S. H. Robertson,[50] A. Lazzaro,[51,52] V. Lombardo,[51] F. Palombo,[51,52] J. M. Bauer,[53] L. Cremaldi,[53] V. Eschenburg,[53] R. Godang,[53,¶] R. Kroeger,[53] D. A. Sanders,[53] D. J. Summers,[53] H. W. Zhao,[53] M. Simard,[54] P. Taras,[54] F. B. Viaud,[54] H. Nicholson,[55] G. De Nardo,[56,57] L. Lista,[56] D. Monorchio,[56,57] G. Onorato,[56,57] C. Sciacca,[56,57] G. Raven,[58] H. L. Snoek,[58] C. P. Jessop,[59] K. J. Knoepfel,[59] J. M. LoSecco,[59] W. F. Wang,[59] G. Benelli,[60] L. A. Corwin,[60] K. Honscheid,[60] H. Kagan,[60] R. Kass,[60] J. P. Morris,[60] A. M. Rahimi,[60] J. J. Regensburger,[60] S. J. Sekula,[60] Q. K. Wong,[60] N. L. Blount,[61] J. Brau,[61] R. Frey,[61] O. Igonkina,[61] J. A. Kolb,[61] M. Lu,[61] R. Rahmat,[61] N. B. Sinev,[61] D. Strom,[61] J. Strube,[61] E. Torrence,[61] G. Castelli,[62,63] N. Gagliardi,[62,63] M. Margoni,[62,63] M. Morandin,[62] M. Posocco,[62] M. Rotondo,[62] F. Simonetto,[62,63] R. Stroili,[62,63] C. Voci,[62,63] P. del Amo Sanchez,[64] E. Ben-Haim,[64] H. Briand,[64] G. Calderini,[64] J. Chauveau,[64] P. David,[64] L. Del Buono,[64] O. Hamon,[64] Ph. Leruste,[64] J. Ocariz,[64] A. Perez,[64] J. Prendki,[64] L. Gladney,[65] M. Biasini,[66,67] R. Covarelli,[66,67] E. Manoni,[66,67] C. Angelini,[68,69] G. Batignani,[68,69] S. Bettarini,[68,69] M. Carpinelli,[68,69,**] A. Cervelli,[68,69] F. Forti,[68,69] M. A. Giorgi,[68,69] A. Lusiani,[68,70] G. Marchiori,[68,69] M. Morganti,[68,69] N. Neri,[68,69] E. Paoloni,[68,69] G. Rizzo,[68,69] J. J. Walsh,[68] J. Biesiada,[71] D. Lopes Pegna,[71] C. Lu,[71] J. Olsen,[71] A. J. S. Smith,[71] A. V. Telnov,[71] F. Anulli,[72] E. Baracchini,[72,73] G. Cavoto,[72] D. del Re,[72,73] E. Di Marco,[72,73] R. Faccini,[72,73] F. Ferrarotto,[72] F. Ferroni,[72,73] M. Gaspero,[72,73] P. D. Jackson,[72] L. Li Gioi,[72] M. A. Mazzoni,[72]

S. Morganti,[72] G. Piredda,[72] F. Polci,[72,73] F. Renga,[72,73] C. Voena,[72] M. Ebert,[74] T. Hartmann,[74] H. Schröder,[74] R. Waldi,[74] T. Adye,[75] B. Franek,[75] E. O. Olaiya,[75] W. Roethel,[75] F. F. Wilson,[75] S. Emery,[76] M. Escalier,[76] L. Esteve,[76] A. Gaidot,[76] S. F. Ganzhur,[76] G. Hamel de Monchenault,[76] W. Kozanecki,[76] G. Vasseur,[76] Ch. Yèche,[76] M. Zito,[76] X. R. Chen,[77] H. Liu,[77] W. Park,[77] M. V. Purohit,[77] R. M. White,[77] J. R. Wilson,[77] M. T. Allen,[78] D. Aston,[78] R. Bartoldus,[78] P. Bechtle,[78] J. F. Benitez,[78] R. Cenci,[78] J. P. Coleman,[78] M. R. Convery,[78] J. C. Dingfelder,[78] J. Dorfan,[78] G. P. Dubois-Felsmann,[78] W. Dunwoodie,[78] R. C. Field,[78] A. M. Gabareen,[78] S. J. Gowdy,[78] M. T. Graham,[78] P. Grenier,[78] C. Hast,[78] W. R. Innes,[78] J. Kaminski,[78] M. H. Kelsey,[78] H. Kim,[78] P. Kim,[78] M. L. Kocian,[78] D. W. G. S. Leith,[78] S. Li,[78] B. Lindquist,[78] S. Luitz,[78] V. Luth,[78] H. L. Lynch,[78] D. B. MacFarlane,[78] H. Marsiske,[78] R. Messner,[78] D. R. Muller,[78] H. Neal,[78] S. Nelson,[78] C. P. O'Grady,[78] I. Ofte,[78] A. Perazzo,[78] M. Perl,[78] B. N. Ratcliff,[78] A. Roodman,[78] A. A. Salnikov,[78] R. H. Schindler,[78] J. Schwiening,[78] A. Snyder,[78] D. Su,[78] M. K. Sullivan,[78] K. Suzuki,[78] S. K. Swain,[78] J. M. Thompson,[78] J. Va'vra,[78] A. P. Wagner,[78] M. Weaver,[78] C. A. West,[78] W. J. Wisniewski,[78] M. Wittgen,[78] D. H. Wright,[78] H. W. Wulsin,[78] A. K. Yarritu,[78] K. Yi,[78] C. C. Young,[78] V. Ziegler,[78] P. R. Burchat,[79] A. J. Edwards,[79] S. A. Majewski,[79] T. S. Miyashita,[79] B. A. Petersen,[79] L. Wilden,[79] S. Ahmed,[80] M. S. Alam,[80] J. A. Ernst,[80] B. Pan,[80] M. A. Saeed,[80] S. B. Zain,[80] S. M. Spanier,[81] B. J. Wogsland,[81] R. Eckmann,[82] J. L. Ritchie,[82] A. M. Ruland,[82] C. J. Schilling,[82] R. F. Schwitters,[82] B. W. Drummond,[83] J. M. Izen,[83] X. C. Lou,[83] F. Bianchi,[84,85] D. Gamba,[84,85] M. Pelliccioni,[84,85] M. Bomben,[86,87] L. Bosisio,[86,87] C. Cartaro,[86,87] G. Della Ricca,[86,87] L. Lanceri,[86,87] L. Vitale,[86,87] V. Azzolini,[88] N. Lopez-March,[88] F. Martinez-Vidal,[88] D. A. Milanes,[88] A. Oyanguren,[88] J. Albert,[89] Sw. Banerjee,[89] B. Bhuyan,[89] H. H. F. Choi,[89] K. Hamano,[89] R. Kowalewski,[89] M. J. Lewczuk,[89] I. M. Nugent,[89] J. M. Roney,[89] R. J. Sobie,[89] T. J. Gershon,[90] P. F. Harrison,[90] J. Ilic,[90] T. E. Latham,[90] G. B. Mohanty,[90] H. R. Band,[91] X. Chen,[91] S. Dasu,[91] K. T. Flood,[91] Y. Pan,[91] M. Pierini,[91] R. Prepost,[91] C. O. Vuosalo,[91] and S. L. Wu[91]

(*BABAR* Collaboration)

[1] *Laboratoire de Physique des Particules, IN2P3/CNRS et Université de Savoie, F-74941 Annecy-Le-Vieux, France*
[2] *Universitat de Barcelona, Facultat de Fisica, Departament ECM, E-08028 Barcelona, Spain*
[3] *INFN Sezione di Bari, I-70126 Bari, Italy*
[4] *Dipartmento di Fisica, Università di Bari, I-70126 Bari, Italy*
[5] *University of Bergen, Institute of Physics, N-5007 Bergen, Norway*
[6] *Lawrence Berkeley National Laboratory and University of California, Berkeley, California 94720, USA*
[7] *University of Birmingham, Birmingham, B15 2TT, United Kingdom*
[8] *Ruhr Universität Bochum, Institut für Experimentalphysik 1, D-44780 Bochum, Germany*
[9] *University of Bristol, Bristol BS8 1TL, United Kingdom*
[10] *University of British Columbia, Vancouver, British Columbia, Canada V6T 1Z1*
[11] *Brunel University, Uxbridge, Middlesex UB8 3PH, United Kingdom*
[12] *Budker Institute of Nuclear Physics, Novosibirsk 630090, Russia*
[13] *University of California at Irvine, Irvine, California 92697, USA*
[14] *University of California at Los Angeles, Los Angeles, California 90024, USA*
[15] *University of California at Riverside, Riverside, California 92521, USA*
[16] *University of California at San Diego, La Jolla, California 92093, USA*
[17] *University of California at Santa Barbara, Santa Barbara, California 93106, USA*
[18] *University of California at Santa Cruz, Institute for Particle Physics, Santa Cruz, California 95064, USA*
[19] *California Institute of Technology, Pasadena, California 91125, USA*
[20] *University of Cincinnati, Cincinnati, Ohio 45221, USA*
[21] *University of Colorado, Boulder, Colorado 80309, USA*
[22] *Colorado State University, Fort Collins, Colorado 80523, USA*
[23] *Technische Universität Dortmund, Fakultät Physik, D-44221 Dortmund, Germany*
[24] *Technische Universität Dresden, Institut für Kern- und Teilchenphysik, D-01062 Dresden, Germany*
[25] *Laboratoire Leprince-Ringuet, CNRS/IN2P3, Ecole Polytechnique, F-91128 Palaiseau, France*
[26] *University of Edinburgh, Edinburgh EH9 3JZ, United Kingdom*
[27] *INFN Sezione di Ferrara, I-44100 Ferrara, Italy*
[28] *Dipartimento di Fisica, Università di Ferrara, I-44100 Ferrara, Italy*
[29] *INFN Laboratori Nazionali di Frascati, I-00044 Frascati, Italy*
[30] *INFN Sezione di Genova, I-16146 Genova, Italy*
[31] *Dipartimento di Fisica, Università di Genova, I-16146 Genova, Italy*
[32] *Harvard University, Cambridge, Massachusetts 02138, USA*
[33] *Universität Heidelberg, Physikalisches Institut, Philosophenweg 12, D-69120 Heidelberg, Germany*

[34]Humboldt-Universität zu Berlin, Institut für Physik, Newtonstr. 15, D-12489 Berlin, Germany

[35]Imperial College London, London, SW7 2AZ, United Kingdom

[36]University of Iowa, Iowa City, Iowa 52242, USA

[37]Iowa State University, Ames, Iowa 50011-3160, USA

[38]Johns Hopkins University, Baltimore, Maryland 21218, USA

[39]Universität Karlsruhe, Institut für Experimentelle Kernphysik, D-76021 Karlsruhe, Germany

[40]Laboratoire de l'Accélérateur Linéaire, IN2P3/CNRS et Université Paris-Sud 11,
Centre Scientifique d'Orsay, B. P. 34, F-91898 Orsay Cedex, France

[41]Lawrence Livermore National Laboratory, Livermore, California 94550, USA

[42]University of Liverpool, Liverpool L69 7ZE, United Kingdom

[43]Queen Mary, University of London, London, E1 4NS, United Kingdom

[44]University of London, Royal Holloway and Bedford New College, Egham, Surrey TW20 0EX, United Kingdom

[45]University of Louisville, Louisville, Kentucky 40292, USA

[46]University of Manchester, Manchester M13 9PL, United Kingdom

[47]University of Maryland, College Park, Maryland 20742, USA

[48]University of Massachusetts, Amherst, Massachusetts 01003, USA

[49]Massachusetts Institute of Technology, Laboratory for Nuclear Science, Cambridge, Massachusetts 02139, USA

[50]McGill University, Montréal, Québec, Canada H3A 2T8

[51]INFN Sezione di Milano, I-20133 Milano, Italy

[52]Dipartimento di Fisica, Università di Milano, I-20133 Milano, Italy

[53]University of Mississippi, University, Mississippi 38677, USA

[54]Université de Montréal, Physique des Particules, Montréal, Québec, Canada H3C 3J7

[55]Mount Holyoke College, South Hadley, Massachusetts 01075, USA

[56]INFN Sezione di Napoli, I-80126 Napoli, Italy

[57]Dipartimento di Scienze Fisiche, Università di Napoli Federico II, I-80126 Napoli, Italy

[58]NIKHEF, National Institute for Nuclear Physics and High Energy Physics, NL-1009 DB Amsterdam, The Netherlands

[59]University of Notre Dame, Notre Dame, Indiana 46556, USA

[60]Ohio State University, Columbus, Ohio 43210, USA

[61]University of Oregon, Eugene, Oregon 97403, USA

[62]INFN Sezione di Padova, I-35131 Padova, Italy

[63]Dipartimento di Fisica, Università di Padova, I-35131 Padova, Italy

[64]Laboratoire de Physique Nucléaire et de Hautes Energies, IN2P3/CNRS, Université Pierre et Marie Curie-Paris6
and Université Denis Diderot-Paris7, F-75252 Paris, France

[65]University of Pennsylvania, Philadelphia, Pennsylvania 19104, USA

[66]INFN Sezione di Perugia, I-06100 Perugia, Italy

[67]Dipartimento di Fisica, Università di Perugia, I-06100 Perugia, Italy

[68]INFN Sezione di Pisa, I-56127 Pisa, Italy

[69]Dipartimento di Fisica, Università di Pisa, I-56127 Pisa, Italy

[70]Scuola Normale Superiore di Pisa, I-56127 Pisa, Italy

[71]Princeton University, Princeton, New Jersey 08544, USA

[72]INFN Sezione di Roma, I-00185 Roma, Italy

[73]Dipartimento di Fisica, Università di Roma La Sapienza, I-00185 Roma, Italy

[74]Universität Rostock, D-18051 Rostock, Germany

[75]Rutherford Appleton Laboratory, Chilton, Didcot, Oxon, OX11 0QX, United Kingdom

[76]DSM/Dapnia, CEA/Saclay, F-91191 Gif-sur-Yvette, France

[77]University of South Carolina, Columbia, South Carolina 29208, USA

[78]Stanford Linear Accelerator Center, Stanford, California 94309, USA

[79]Stanford University, Stanford, California 94305-4060, USA

[80]State University of New York, Albany, New York 12222, USA

[81]University of Tennessee, Knoxville, Tennessee 37996, USA

[82]University of Texas at Austin, Austin, Texas 78712, USA

[83]University of Texas at Dallas, Richardson, Texas 75083, USA

[*]Deceased.

[+]Now at Temple University, Philadelphia, Pennsylvania 19122, USA.

[‡]Now at Tel Aviv University, Tel Aviv, 69978, Israel.

[§]Also with Università di Perugia, Dipartimento di Fisica, Perugia, Italy.

[‖]Also with Università di Roma La Sapienza, I-00185 Roma, Italy.

[¶]Now at University of South Alabama, Mobile, Alabama 36688, USA.

[**]Also with Università di Sassari, Sassari, Italy.

[84]*INFN Sezione di Torino, I-10125 Torino, Italy*
[85]*Dipartimento di Fisica Sperimentale, Università di Torino, I-10125 Torino, Italy*
[86]*INFN Sezione di Trieste, I-34127 Trieste, Italy*
[87]*Dipartimento di Fisica, Università di Trieste, I-34127 Trieste, Italy*
[88]*IFIC, Universitat de Valencia-CSIC, E-46071 Valencia, Spain*
[89]*University of Victoria, Victoria, British Columbia, Canada V8W 3P6*
[90]*Department of Physics, University of Warwick, Coventry CV4 7AL, United Kingdom*
[91]*University of Wisconsin, Madison, Wisconsin 53706, USA*
(Received 30 June 2008; published 15 September 2008)

We report the results of a search for the decay $B^0 \to K^{*+}K^{*-}$ with a sample of 454 ± 5 million $B\bar{B}$ pairs collected with the *BABAR* detector at the PEP-II asymmetric-energy e^+e^- collider at the Stanford Linear Accelerator Center. We obtain an upper limit at the 90% confidence level on the branching fraction for $\mathcal{B}(B^0 \to K^{*+}K^{*-}) < 2.0 \times 10^{-6}$, assuming the decay is fully longitudinally polarized.

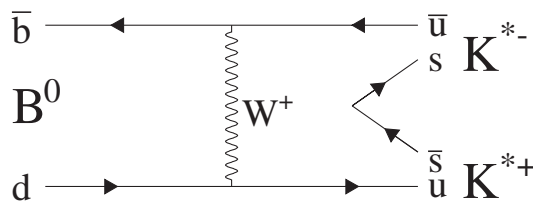The study of the branching fractions and angular distributions of B meson decays to hadronic final states without a charm quark probes the dynamics of both weak and strong interactions and plays an important role in understanding CP violation. Improved experimental measurements of these charmless decays, combined with theoretical developments, can provide significant constraints on the Cabibbo-Kobayashi-Maskawa matrix parameters [1] and uncover evidence for physics beyond the standard model [2,3].

QCD factorization models predict the angular distribution of the decay of the B meson to two vector particles (VV), as measured by the longitudinal polarization fraction f_L, to be ~0.9 for both tree- and penguin-dominated decays [4]. Two measurements of the pure penguin VV decay $B \to \phi K^*$ give $f_L = 0.52 \pm 0.08 \pm 0.03$ and $f_L = 0.49 \pm 0.05 \pm 0.03$ [5], while $f_L = 0.81^{+0.10}_{-0.12} \pm 0.06$ has recently been measured for the decay $B^0 \to K^{*0}\bar{K}^{*0}$ [6]. Several attempts to understand the values of f_L within or beyond the standard model have been made [7]. Further information about decays related by $SU(3)$ symmetry may provide insights into this polarization puzzle and test factorization models.

The decay $B^0 \to K^{*+}K^{*-}$ is expected to occur through a $b \to u$ quark transition via W-exchange, as shown in Fig. 1, or from final-state interactions. Its branching fraction is expected to be small, with Beneke, Rohrer, and Yang [2] predicting $(0.09^{+0.05+0.12}_{-0.03-0.10}) \times 10^{-6}$, while Cheng and Yang [3] quote $(0.1 \pm 0.0 \pm 0.1) \times 10^{-6}$, both based on QCD factorization. The current experimental upper

limit on the branching fraction at the 90% confidence level (C.L.) is $141(89) \times 10^{-6}$ [8], assuming a fully longitudinally (transversely) polarized system. Searches for the related decay $B^0 \to K^+K^-$ have produced upper limits on the branching fraction at the 90% C.L. in the range $(0.4{-}0.8) \times 10^{-6}$ [9].

We report on a search for the decay mode $B^0 \to K^{*+}K^{*-}$, where $K^{*\pm}$ refers to the $K^{*\pm}(892)$ resonance, without explicit consideration of interference from higher mass K^* states, and place an upper limit on the branching fraction. Charge-conjugate modes are implied throughout and we assume equal production rates of B^+B^- and $B^0\bar{B}^0$.

This analysis is based on a data sample of 454 ± 5 million $B\bar{B}$ pairs, corresponding to an integrated luminosity of 413 fb^{-1}, collected with the *BABAR* detector at the PEP-II asymmetric-energy e^+e^- collider operated at the Stanford Linear Accelerator Center. The e^+e^- center-of-mass (c.m.) energy is $\sqrt{s} = 10.58$ GeV, corresponding to the $Y(4S)$ resonance mass (on-resonance data). In addition, 41.2 fb^{-1} of data collected at 40 MeV below the $Y(4S)$ resonance (off-resonance data) are used for background studies.

The *BABAR* detector is described in detail in Ref. [10]. Charged particles are reconstructed as tracks with a 5-layer silicon vertex detector and a 40-layer drift chamber inside a 1.5-T solenoidal magnet. An electromagnetic calorimeter (EMC) comprising 6580 CsI(Tl) crystals is used to identify electrons and photons. A ring-imaging Cherenkov detector (DIRC) is used to identify charged hadrons and to provide additional electron identification information. The average K-π separation in the DIRC varies from 12σ at a laboratory momentum of 1.5 GeV/c to 2.5σ at 4.5 GeV/c. Muons are identified by an instrumented magnetic-flux return (IFR).

The $B^0 \to K^{*+}K^{*-}$ candidates are reconstructed through the decay of both $K^{*\pm}$ to $K^0_S\pi^\pm$ or with one $K^{*\pm}$ decaying to $K^0_S\pi^\pm$ and the other to $K^\mp\pi^0$. The differential decay rate, after integrating over the angle between the decay planes of the vector mesons, for which the acceptance is uniform, is

FIG. 1.   The $b \to u$ W-exchange diagram for $B^0 \to K^{*+}K^{*-}$.

$$\frac{1}{\Gamma}\frac{d^2\Gamma}{d\cos\theta_1 d\cos\theta_2} \propto \frac{1-f_L}{4}\sin^2\theta_1\sin^2\theta_2 + f_L\cos^2\theta_1\cos^2\theta_2, \quad (1)$$

where θ_1 and θ_2 are the helicity angles of the K^{*+} and K^{*-}, defined as the angle between the daughter kaon (K_S^0 or $K^{\pm}$) momentum and the direction opposite to the B meson in the $K^{*\pm}$ rest frame [11].

The charged particles from the $K^{*\pm}$ decays are required to have at least 12 hits in the drift chamber and a transverse momentum greater than 0.1 GeV/c. The particles are identified as either charged pions or kaons by measurement of the energy loss in the tracking devices, the number of photons recorded by the DIRC, and the corresponding Cherenkov angle. These measurements are combined with additional information from the EMC and IFR detectors, where appropriate, to reject electrons, muons, and protons.

The K_S^0 is reconstructed through its decay to $\pi^+\pi^-$. The K_S^0 candidates are required to have a reconstructed mass within 0.01 GeV/c^2 of the nominal K_S^0 mass [12], a decay vertex separated from the B meson vertex by at least 20 times the uncertainty in the measurement of the vertex position, a flight distance in the transverse direction of at least 0.3 cm, and the cosine of the angle between the line joining the B and K_S^0 decay vertices and the K_S^0 momentum greater than 0.999.

We reconstruct the π^0 through the decay $\pi^0 \to \gamma\gamma$. In the laboratory frame, the energy of each photon from the π^0 candidate must be greater than 0.04 GeV, the energy of the π^0 must be greater than 0.25 GeV, and the reconstructed π^0 invariant mass is required to be $0.12 \le m_{\gamma\gamma} \le 0.15$ GeV/c^2.

We require the invariant mass of the K^{*+} candidates to be $0.792 < m_{K\pi} < 0.992$ GeV/c^2. A B meson candidate is formed from the $K^{*\pm}$ candidates, with the condition that the $K^{*\pm}$ candidates originate from the interaction region.

B meson candidates are characterized kinematically by the energy difference $\Delta E = E_B^* - \sqrt{s}/2$ and the beam energy-substituted mass $m_{\mathrm{ES}} = [(s/2 + \mathbf{p}_i \cdot \mathbf{p}_B)^2/E_i^2 - \mathbf{p}_B^2]^{1/2}$, where $(E_i, \mathbf{p}_i)$ and $(E_B, \mathbf{p}_B)$ are the four-momenta of the $\Upsilon(4S)$ and B meson candidate, respectively, and the asterisk denotes the $\Upsilon(4S)$ rest frame. For a final state with a π^0, the total event sample is taken from the region $-0.1 \le \Delta E \le 0.2$ GeV and $5.25 \le m_{\mathrm{ES}} \le 5.29$ GeV/c^2; with no π^0, the signal ΔE has a smaller width and the region $-0.08 \le \Delta E \le 0.15$ GeV is used. The asymmetric ΔE criteria are applied to remove backgrounds from charm decays which occur in the negative ΔE region. In both cases, events outside the region $|\Delta E| \le 0.07$ GeV and $5.27 \le m_{\mathrm{ES}} \le 5.29$ GeV/c^2 are used to characterize the background.

We suppress the background from decays to charmed states by forming the invariant mass, m_D, from combina-

tions of three out of the four daughter particles' four-momenta. The event is rejected if $1.845 < m_D < 1.895$ GeV/c^2 and the charge and particle type of the tracks are consistent with a decay from a D meson. We reduce backgrounds from $B^0 \to \phi K^{*0}$ by assigning the kaon mass to the pion candidate and rejecting the event if the combined invariant mass of the two charged tracks is between 1.00 and 1.04 GeV/c^2. Finally, to reduce the continuum background and avoid the region where the reconstruction efficiency falls off rapidly for low momentum tracks, we require the cosine of the helicity angle of the $K^{*\pm}$ candidates to be in the range $-1.0 \le \cos(\theta) \le 0.9$ for states without a π^0 and $-0.9 \le \cos(\theta) \le 0.9$ for decays with a π^0.

To reject the dominant background consisting of light-quark $q\bar{q}(q = u, d, s, c)$ continuum events, we require $|\cos\theta_T| < 0.8$, where θ_T is the angle, in the c.m. frame, between the thrust axis [13] of the B meson and that formed from the other tracks and neutral clusters in the event. Signal events have a flat distribution in $|\cos\theta_T|$, while continuum events peak at 1.

We use Monte Carlo (MC) simulations of the signal decay to estimate the number of signal candidates per event. After the application of the selection criteria, the average number of signal candidates per event is predicted to be 1.08 (1.02) for fully longitudinally (transversely) polarized decays with no π^0 in the final state and 1.18 (1.10) for decays with one π^0 in the final state. A single candidate per event is chosen as the one whose fitted decay vertex has the smallest χ^2. MC simulations also show that up to 7% (2.4%) of longitudinally (transversely) polarized signal events with no π^0 are misreconstructed, with one or more tracks originating from the other B meson in the event. In the case of signal events with one π^0, the number of misreconstructed candidates is 11% (4.3%) for longitudinally (transversely) polarized signal events.

We create a Fisher discriminant $\mathcal{F}$ to be used in the maximum-likelihood (ML) fit, constructed from a linear combination of five variables: the polar angles of the B meson momentum vector and the B meson thrust axis with respect to the beam axis, the ratio of the second- and zeroth-order momentum-weighted Legendre polynomial moments of the energy flow around the B meson thrust axis in the c.m. frame [14], the flavor of the other B meson as reported by a multivariate tagging algorithm [15], and the boost-corrected proper-time difference between the decays of the two B mesons divided by its variance. The second B meson is formed by creating a vertex from the remaining tracks that are consistent with originating from the interaction region. The Fisher discriminant is trained using MC for signal and $q\bar{q}$ continuum MC, off-resonance data and data outside the signal region for the background.

We use an extended unbinned ML fit to extract the signal yield and polarization simultaneously for each mode. The extended likelihood function is

$$\mathcal{L} = \frac{1}{N!} \exp\left(-\sum_j n_j\right) \prod_{i=1}^{N} \left[\sum_j n_j \mathcal{P}_j(\vec{x}_i; \vec{\alpha}_j)\right]. \quad (2)$$

We define the likelihood $\mathcal{L}_i$ for each event candidate i as the sum of $n_j \mathcal{P}_j(\vec{x}_i; \vec{\alpha}_j)$ over three hypotheses j (signal, $q\bar{q}$ background and $B\bar{B}$ backgrounds as discussed below), where $\mathcal{P}_j(\vec{x}_i; \vec{\alpha}_j)$ is the product of the probability density functions (PDFs) for hypothesis j evaluated for the ith event's measured variables $\vec{x}_i$, n_j is the yield for hypothesis j, and N is the total number of events in the sample. The quantities $\vec{\alpha}_j$ represent parameters in the expected distributions of the measured variables for each hypothesis j. Each discriminating variable $\vec{x}_i$ in the likelihood function is modeled with a PDF, where the parameters $\vec{\alpha}_j$ are extracted from MC simulation, off-resonance data, or (m_{ES}, ΔE) sideband data.

The seven variables $\vec{x}_i$ used in the fit are m_{ES}, ΔE, $\mathcal{F}$, and the invariant masses and cosines of the helicity angle of the two $K^{*\pm}$ candidates. Since the correlations among the fitted input variables are found to be on average $\sim 1\%$, with a maximum of 5%, we take each $\mathcal{P}_j$ to be the product of the PDFs for the separate variables. The effect of neglecting correlations is evaluated by fitting ensembles of simulated experiments in which we embed signal and background events randomly extracted from fully simulated MC samples. Any observed fit bias is then subtracted from the fitted yield.

For the final state with no π^0, the two-invariant mass and helicity angle distributions for each $K^{*\pm}$ meson are indistinguishable and so we use the same PDF parameters for both $K^{*\pm}$ candidates; for the final state with a π^0, we use separate PDFs for $K^{*\pm} \to K_S^0 \pi^\pm$ and $K^{*\mp} \to K^\mp \pi^0$. For the signal, we use a relativistic Breit-Wigner for the $K^{*\pm}$ invariant mass and a sum of two Gaussians for m_{ES} and ΔE. The longitudinal (transverse) helicity angle distributions are described with a $\cos^2\theta$ ($\sin^2\theta$) function corrected for changes in efficiency as a function of helicity angle. The correction also accounts for the reduction in efficiency at a helicity of ~ 0.78 introduced indirectly by the criteria used to veto D mesons. The $B\bar{B}$ backgrounds use an empirical nonparametric function for ΔE, the masses and helicity angles. The continuum and the $B\bar{B}$ background m_{ES} shapes are described by the function $x\sqrt{1-x^2}\exp[-\xi(1-x^2)]$ (with $x = m_{\mathrm{ES}}/E_B^*$ and ξ a free parameter) [16] and a first- or third-order polynomial is used for ΔE and the helicity angles, respectively. The continuum invariant mass distributions contain real $K^{*\pm}$ candidates; we model the peaking mass component using the parameters extracted from the fit to the signal invariant mass distributions together with a second-order polynomial to represent the nonpeaking component. The Fisher distributions are modeled using an asymmetric Gaussian for all hypotheses.

$B\bar{B}$ backgrounds that remain after the event selection criteria have been applied are identified and modeled using

MC simulation based on the full physics and detector models [17]. There are no significant charmless $B\bar{B}$ backgrounds. The charm $B\bar{B}$ backgrounds are effectively suppressed by applying the veto on D meson mass described above. The remaining charm $B\bar{B}$ background events are mostly single candidates formed from the decay products of a D, D^*, or $D_s^{*\pm}$, together with another track from the event. Given the uncertainty in the polarization and branching fractions of these backgrounds, we allow the $B\bar{B}$ background yield to float in the fit.

The continuum background PDF parameters that are allowed to vary are the $\mathcal{F}$ peak position, ξ for m_{ES}, the slope of ΔE, and the polynomial coefficients and normalizations describing the mass and helicity angle distributions. We fit for the branching fraction $\mathcal{B}$ and f_L directly and exploit the fact that $\mathcal{B}$ is less correlated with f_L than is either the yield or efficiency taken separately. We validate the fitting procedure and extract fitting biases by applying the fit to ensembles of simulated experiments using the extracted fitted yields from data. The $q\bar{q}$ component is drawn from the PDF, and the signal and $B\bar{B}$ background events are randomly sampled from the fully simulated MC samples.

The total event sample consists of 602 and 1923 events for $B^0 \to K^{*+} K^{*-}$ with zero or one π^0 in the final state, respectively. The corresponding signal event yield is $1.8^{+2.7}_{-1.7}$ and $4.1^{+5.8}_{-3.2}$ and the longitudinal polarization f_L is 0.0 ± 0.6 and 1.0 ± 1.0, respectively. Given the large errors on f_L, we repeat the analysis with f_L set to 1.0; this gives the most conservative 90% confidence level upper limit on the branching fractions. The results of the ML fits with $f_L = 1.0$ are summarized in Table I. The $B\bar{B}$ back-

TABLE I. Summary of results with $f_L = 1.0$ for the fitted yields, fit biases, reconstruction efficiencies ϵ, sub-branching fractions $\prod \mathcal{B}_i$, branching fraction $\mathcal{B}$ ($B^0 \to K^{*+} K^{*-}$), significance S, and 90% C.L. upper limit $\mathcal{B}_{\mathrm{UL}}$. The first error is statistical and the second, if given, is systematic.

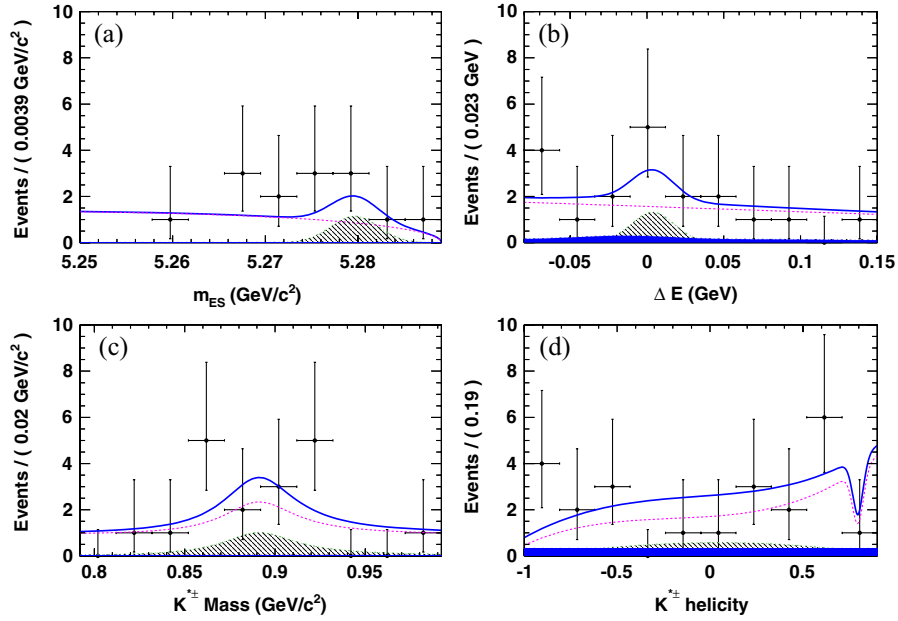| Final state	$K_S^0\pi^+ K_S^0\pi^-$	$K_S^0\pi^\pm K^\mp\pi^0$
Yields (events):		
Total	602	1923
Signal	$0.7^{+2.5}_{-1.4}$	$4.2^{+4.6}_{-3.3}$
$B\bar{B}$ bkg.	20 ± 20	84 ± 51
$q\bar{q}$ bkg.	580 ± 25	1835 ± 70
ML fit biases	-0.170	1.70
Efficiencies and $\mathcal{B}$:		
$\epsilon(\%)$	8.89 ± 0.08	4.83 ± 0.04
$\prod \mathcal{B}_i(\%)$	5.32	15.19
$\mathcal{B}$ ($\times 10^{-6}$)	$0.38^{+1.1}_{-0.6} \pm 0.05$	$0.76^{+1.4}_{-1.0} \pm 0.16$
Significance S (σ)	0.50	0.74
Combined results:		
$\mathcal{B}$ ($\times 10^{-6}$)	$0.52^{+0.83+0.08}_{-0.58-0.06}$	
Significance S (σ)	0.87	
$\mathcal{B}_{\mathrm{UL}}$ ($\times 10^{-6}$)	2.0	

FIG. 2 (color online). Projections of the multidimensional fit onto (a) m_{ES}; (b) ΔE; (c) $K^{*\pm}$ mass; and (d) cosine of $K^{*\pm}$ helicity angle for $B^0 \to K^{*\pm}(\to K^0_S \pi^{\pm})K^{*\mp}(\to K^0_S \pi^{\mp})$ events selected with a requirement on the signal-to-total likelihood probability ratio, optimized for each variable, with the plotted variable excluded. The points with error bars show the data; the solid line shows signal-plus-background; the dashed line is the continuum background; the hatched region is the signal; and the shaded region is the $B\bar{B}$ background.

ground yield agrees with the MC prediction within the large statistical errors. We compute the branching fractions $\mathcal{B}$ by subtracting the ML fit bias from the fitted yield and dividing the result by the number of $B\bar{B}$ pairs and by the reconstruction efficiency, ϵ, times $\mathcal{B}(K^0 \to K^0_S \to \pi^+\pi^-) = 0.5 \times (69.20 \pm 0.05)\%$ and $\mathcal{B}(\pi^0 \to \gamma\gamma) =$

$(98.80 \pm 0.03)\%$. The significance S of the signal is defined as $S = 2\Delta\ln\mathcal{L}$, where $\Delta\ln\mathcal{L}$ is the change in likelihood from the maximum value when the number of signal events is set to zero, corrected for the systematic errors defined below.
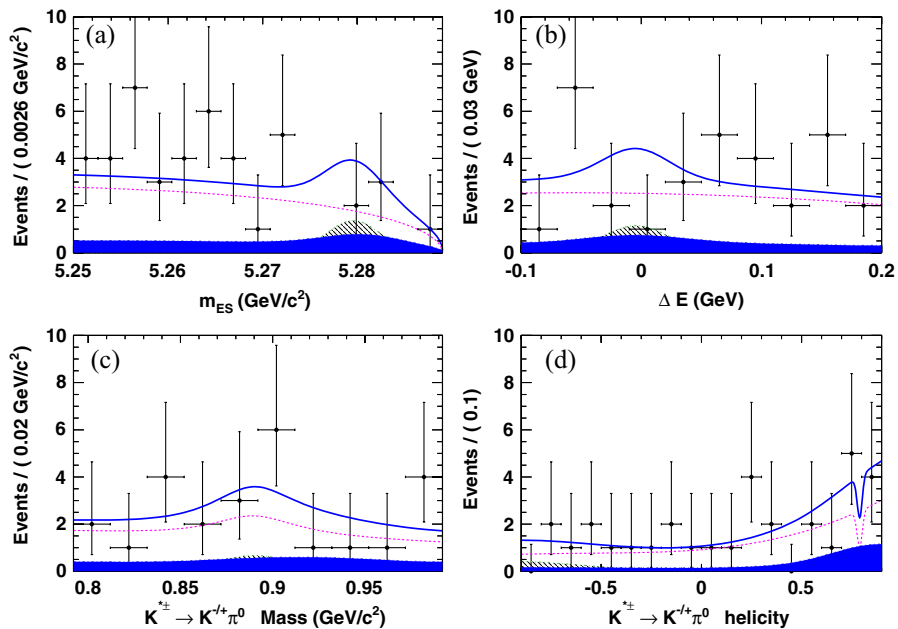

FIG. 3 (color online). Projections of the multidimensional fit onto (a) m_{ES}; (b) ΔE; (c) $K^{*\pm}$ mass; and (d) cosine of $K^{*\pm}$ helicity angle for $B^0 \to K^{*\pm}(\to K^0_S \pi^{\pm})K^{*\mp}(\to K^{\mp} \pi^0)$. The same projection criteria and legend are used as in Fig. 2.

The significance of the $B^0 \to K^{*+}K^{*-}$ branching fraction is 0.87σ, including statistical and systematic uncertainties. The 90% C.L. branching fraction upper limit ($\mathcal{B}_{\mathrm{UL}}$) is determined by combining the likelihoods from the two fits and integrating the total likelihood distribution (taking into account correlated and uncorrelated systematic uncertainties) as a function of the branching fraction from 0 to $\mathcal{B}_{\mathrm{UL}}$, so that $\int_0^{\mathcal{B}_{\mathrm{UL}}} \mathcal{L} d\mathcal{B} = 0.9 \int_0^\infty \mathcal{L} d\mathcal{B}$.

Figures 2 and 3 show the projections of the two fits onto m_{ES}, ΔE, $K^{*\pm}$ mass and cosine of the $K^{*\pm}$ helicity angle for the final state with zero and one π^0, respectively. The candidates in the figures are signal-enhanced with a requirement on the probability ratio $\mathcal{P}_{\mathrm{sig}}/(\mathcal{P}_{\mathrm{sig}} + \mathcal{P}_{\mathrm{bkg}})$, optimized to enhance the visibility of potential signal, where $\mathcal{P}_{\mathrm{sig}}$ and $\mathcal{P}_{\mathrm{bkg}}$ are the signal and the total background probabilities, respectively, (computed without using the variable plotted). The dip in helicity at ~ 0.78 is created by the criteria used to veto charm background.

The systematic uncertainties are summarized in Table II. The errors on the branching fractions arise from the PDFs, fit biases, and efficiencies. The PDF uncertainties are calculated by varying the PDF parameters that are held fixed in the original fit by their errors. The uncertainty from the fit bias includes its statistical uncertainty from the simulated experiments and half of the correction itself, added in quadrature. The uncertainties in PDF modeling and fit bias are additive in nature and affect the significance of the branching fraction results. Multiplicative uncertainties include reconstruction efficiency uncertainties from tracking and particle identification (PID), track multiplicity, MC signal efficiency statistics, and the number of $B\bar{B}$ pairs.

In summary, we have measured the branching fraction $\mathcal{B}(B^0 \to K^{*+}K^{*-}) = [0.52^{+0.83+0.08}_{-0.58-0.06}] \times 10^{-6}$, assuming the decay is fully longitudinally polarized. The 90% C.L. upper limit on the branching fraction $\mathcal{B}(B^0 \to K^{*+}K^{*-}) < 2.0 \times 10^{-6}$ is nearly 2 orders of magnitude more stringent than previous searches.

TABLE II. Estimated systematic errors in the final fit. Error sources which are correlated and uncorrelated when combined from the two decays are denoted by C and U, respectively.

Final state	$K_S^0\pi^+ K_S^0\pi^-$	$K_S^0\pi^+ K^\pm\pi^0$
Additive errors (events)		
Fit bias [U]	0.09	0.85
Fit parameters [U]	0.06	0.25
Total additive (events)	0.10	0.88
Multiplicative errors (%)		
Track multiplicity [C]	1.0	1.0
MC statistics [U]	0.5	0.6
Number of $B\bar{B}$ pairs [C]	1.1	1.1
PID [C]	2.2	1.1
Neutrals corrections [C]	—	3.0
K_S^0 corrections [C]	1.8	1.4
Tracking corrections [C]	1.6	0.8
Total multiplicative (%)	3.6	3.9
Total $\mathcal{B}$ error ($\times 10^{-6}$)	0.05	0.16

[1] N. Cabibbo, Phys. Rev. Lett. **10**, 531 (1963); M. Kobayashi and T. Maskawa, Prog. Theor. Phys. **49**, 652 (1973).

[2] M. Beneke, J. Rohrer, and D. Yang, Nucl. Phys. **B774**, 64 (2007).

[3] H. Y. Cheng and K. C. Yang, arXiv:0805.0329v1.

[4] A. Ali *et al.*, Z. Phys. C **1**, 269 (1979); M. Suzuki, Phys. Rev. D **66**, 054018 (2002).

[5] K.-F. Chen *et al.* (Belle Collaboration), Phys. Rev. Lett. **94**, 221804 (2005); B. Aubert *et al.* (*BABAR* Collaboration), Phys. Rev. Lett. **99**, 201802 (2007).

[6] B. Aubert *et al.* (*BABAR* Collaboration), Phys. Rev. Lett. **100**, 081801 (2008).

[7] A. Kagan, Phys. Lett. B **601**, 151 (2004); C. Bauer *et al.*, Phys. Rev. D **70**, 054015 (2004); P. Colangelo *et al.*, Phys. Lett. B **597**, 291 (2004); M. Ladisa *et al.*, Phys. Rev. D **70**, 114025 (2004); H.-n. Li and S. Mishima, Phys. Rev. D **71**, 054025 (2005); M. Beneke *et al.*, Phys. Rev. Lett. **96**,

141801 (2006).

[8] R. Godang *et al.* (CLEO Collaboration), Phys. Rev. Lett. **88**, 021802 (2001).

[9] B. Aubert *et al.* (*BABAR* Collaboration), Phys. Rev. D **75**, 012008 (2007); S.-W. Lin *et al.* (Belle Collaboration), Phys. Rev. Lett. **98**, 181804 (2007); A. Bornheim *et al.* (CLEO Collaboration), Phys. Rev. D **68**, 052002 (2003).

[10] B. Aubert *et al.* (*BABAR* Collaboration), Nucl. Instrum. Methods Phys. Res., Sect. A **479**, 1 (2002).

[11] G. Kramer and W. F. Palmer, Phys. Rev. D **45**, 193 (1992).

[12] W.-M. Yao *et al.* (Particle Data Group), J. Phys. G **33**, 1

(2006).

[13] S. Brandt *et al.*, Phys. Lett. **12**, 57 (1964); E. Farhi, Phys. Rev. Lett. **39**, 1587 (1977).

[14] B. Aubert *et al.* (*BABAR* Collaboration), Phys. Rev. D **70**, 032006 (2004).

[15] B. Aubert *et al.* (*BABAR* Collaboration), Phys. Rev. Lett. **89**, 201802 (2002).

[16] H. Albrecht *et al.* (ARGUS Collaboration), Phys. Lett. B **241**, 278 (1990).

[17] S. Agostinelli *et al.* (GEANT Collaboration), Nucl. Instrum. Methods Phys. Res., Sect. A **506**, 250 (2003).